

Structural Critical Scattering Study of Mg-Doped CuGeO₃

Y. J. Wang, V. Kiryukhin, and R. J. Birgeneau

Department of Physics, Massachusetts Institute of Technology, Cambridge, Massachusetts 02139

T. Masuda, I. Tsukada, and K. Uchinokura

Department of Applied Physics, The University of Tokyo, 7-3-1 Hongo, Bunkyo-ku, Tokyo 113-8656, Japan

(Received 11 January 1999)

We report a synchrotron x-ray scattering study of the diluted spin-Peierls (SP) material Cu_{1-x}Mg_xGeO₃. We find that for $x > 0$ the temperature T_m at which the spin gap is established is significantly higher than the temperature T_s at which the SP dimerization attains long-range order. The latter is observed only for $x < x_c \sim 0.021$, while for $x > x_c$ the SP correlation length quickly decreases with increasing x . We argue that impurity-induced competing interchain interactions play a central role in these phenomena.

PACS numbers: 75.30.Kz, 75.10.Jm, 75.40.Cx, 75.80.+q

Low-dimensional quantum spin systems exhibit a variety of intriguing and often counterintuitive properties. A prominent example of such a material is the spin-Peierls (SP) system [1] which consists of an array of one-dimensional (1D) antiferromagnetic spin chains with $S = \frac{1}{2}$ on a deformable 3D lattice. Below the spin-Peierls transition temperature, T_{SP} , the spin chains dimerize and a gap opens in the magnetic excitation spectrum. The discovery of an inorganic SP compound CuGeO₃ (Ref. [2]) made possible a systematic study of impurity effects on SP systems [3]. In CuGeO₃, Zn²⁺, Mg²⁺ ($S = 0$), and Ni²⁺ ($S = 1$) can be substituted for Cu²⁺ ($S = \frac{1}{2}$) thus directly affecting the spin chains [4,5]. A variety of unexpected phenomena that cannot be explained by a simple dilution effect were quickly discovered in impurity-doped CuGeO₃ [4–8]. At present, a comprehensive theoretical description of the T - x phase diagram of impurity-doped CuGeO₃ still remains to be established.

Despite the extensive amount of work on doped CuGeO₃, the phase diagram of this system is still not fully established and remains controversial, especially at large doping. Notably, there is a disagreement between the results obtained by different experimental techniques. In Cu_{1-x}Zn_xGeO₃, for instance, the SP transition appears to vanish above $x \sim 0.02$ as evidenced by magnetic susceptibility measurements [3], but appreciable lattice dimerization is still observed at $x = 0.047$ in neutron diffraction experiments [8]. Diffraction measurements also show that at large x the SP state does not attain long-range order (LRO) in the case of Zn and Ni doping [7,8], but no systematic data are available. Recently, Masuda *et al.* [5] reported magnetic susceptibility measurements indicating that the Mg-doped material undergoes a first order transition as a function of x at $x_c \sim 0.023$. According to Ref. [5], the SP transition abruptly disappears at x_c . This basic scenario has been confirmed by Nakao *et al.* [9] using neutron diffraction techniques; however, they argue that $x_c = 0.027 \pm 0.001$ and that broadened

SP dimerization peaks are still present for $x > x_c$ in Cu_{1-x}Mg_xGeO₃. It is evident that a reliable determination of the SP transition temperature T_{SP} is of crucial importance. A second order phase transition temperature is typically defined as the temperature at which the correlation length diverges and LRO is achieved in the system. Therefore, to resolve the current controversy on the phase diagram of doped CuGeO₃ and to elucidate the underlying physics, application of an experimental technique such as high resolution synchrotron x-ray scattering which probes with high precision any possible long-range structural order is needed.

In this paper, we report a synchrotron x-ray scattering study of the temperature-doping phase diagram of Cu_{1-x}Mg_xGeO₃. We find the surprising result that, except for the pure compound, the temperature T_s at which the SP dimerization attains LRO is significantly lower than the temperature T_m at which both short-range order SP dimerization diffraction peaks appear *and* a local spin gap is established [10]. The opening of the magnetic gap is deduced from the susceptibility measurements of Ref. [5]. We argue that the structural properties of doped CuGeO₃ are determined by impurity-induced competing interchain interactions and, possibly, random fields, and therefore are similar to the properties of other systems with competing interactions and/or fields, such as spin glasses and random field Ising model (RFIM) compounds. These random competing interchain interactions naturally produce significant differences in the local and long-range ordering temperatures. The SP LRO is observed only for $x < x_c$ with $x_c \leq 0.021$. In fact, in this paper we define x_c using this criterion; see also Ref. [11]. For $x > x_c$, the SP correlation length quickly decreases and the SP peaks weaken with increasing x . Thus, in agreement with the hypothesis in Ref. [5], the SP transition is absent for $x > x_c$.

The experiment was carried out at MIT-IBM beam line X20A at the National Synchrotron Light Source. The 8.5 keV x-ray beam was focused by a mirror,

monochromatized by a pair of Ge (111) crystals, scattered from the sample, and analyzed by a Si (111) analyzer. High quality [11] $\text{Cu}_{1-x}\text{Mg}_x\text{GeO}_3$ single crystals (0.01° – 0.02° mosaic width) from the same batches as those studied in [5] with x varying from zero to 0.035 were used. Carefully cleaved samples were placed inside a Be can filled with helium heat-exchange gas and mounted on the cold finger of a 4 K closed cycle cryostat. The experiment was carried out around the (1.5, 1, 1.5) SP dimerization peak position with the $(H K H)$ zone in the scattering plane. The highest intrinsic correlation length measurable in our experiment was about $0.5 \mu\text{m}$ (5000 \AA); we considered that a sample possessed LRO if the correlation length exceeded this value since significantly larger lengths are essentially macroscopic.

A representative set of longitudinal (parallel to the scattering vector) x-ray scans at the (1.5, 1, 1.5) SP dimerization peak position for $x = 0.017$, 0.0237, and 0.026 samples at various temperatures is shown in Fig. 1. The low-temperature SP peak intensity in the $x = 0.017$ sample was 4×10^4 counts/s with a background of 10 counts/s. The low-temperature SP peak width is resolution limited in the $x = 0.017$ sample, indicating that the SP state possesses LRO. On the other hand, the SP peaks in the $x = 0.0237$ and $x = 0.026$ samples are broadened at all experimentally accessible temperatures, and therefore only short-range order is present. To extract the intrinsic correlation length, the data for all samples were fitted to a two-dimensional convolution (longitudinal and transverse directions) of the experimentally measured Gaussian resolution function with the intrinsic cross section (Lorentzian line shapes taken to various powers were attempted). The intensity was automatically integrated over the third direction due to our experimental setup. A presumed 3D Lorentzian-squared intrinsic line shape resulted in the best fits; they are shown as the solid lines in Fig. 1. The Lorentzian-squared cross section is characteristic of 3D systems with quenched randomness [12], thus indicating that randomness plays a central role in the phase behavior in the doped SP samples.

Figure 2(a) shows the temperature dependence of the (1.5, 1, 1.5) dimerization peak intensity for various doped samples. The data are normalized to the corresponding (1, 0, 1) Bragg peak intensity. In contrast to the case of pure CuGeO_3 , the transitions are noticeably rounded with the rounding increasing with increasing x [13]. Such a substantial rounding cannot be explained by local concentration gradients since the doping is too low to create any correlated effect. The inset of Fig. 2(a) shows the maximum SP peak intensity as a function of doping x . The peak intensity abruptly decreases around $x \sim 0.025$, which is roughly the doping level at which the SP dip in susceptibility measurements is reported to disappear [5]. Figure 2(b) shows the temperature dependence of the longitudinal inverse correlation length. The low-temperature inverse correlation length as a function of x is shown in the

inset. The system attains LRO only for $x < x_c \leq 0.021$. While substantial intensity is still observed at the SP peak position for $x > x_c$, the system has only short-range SP order. Therefore, the phase transition as a function of x reported by Masuda *et al.* [5] is characterized by the loss of SP LRO at the critical doping x_c . As noted previously, a similar conclusion has been reached by Nakao *et al.* albeit with $x_c \sim 0.027$; we believe that their results are consistent with ours and that the difference in the deduced values for x_c originates primarily in the much higher resolution of our synchrotron x-ray study compared with the neutron diffraction experiments. As discussed in Ref. [11], other anomalies observed by Nakao *et al.* [9] for $x \sim 0.027$ are connected with the termination of the pseudo-two-phase coexistence region of the Néel state.

A central observation of this work is illustrated in Fig. 3 which presents data for the $x = 0.021$ sample. This sample attains LRO at low temperatures. Figure 3 shows the temperature dependences of the SP peak intensity, the intensity at the wing of the SP peak, and the corresponding longitudinal intrinsic peak width. A phase transition temperature is properly defined as the temperature at which the correlation length of the order parameter fluctuations diverges. It is evident from the data of Fig. 3 that the temperature at which the LRO is achieved in this sample is noticeably lower than both the onset temperature at which significant intensity is observable at the SP peak position and the temperature at which the wing intensity shows a peak. Moreover, magnetic susceptibility and neutron diffraction measurements give an even higher apparent SP transition temperature $T_{\text{SP}} \sim 11 \text{ K}$ [5,9]. The discrepancy between the neutron and x-ray diffraction measurements can again be understood by taking into account the moderate momentum-space resolution of the

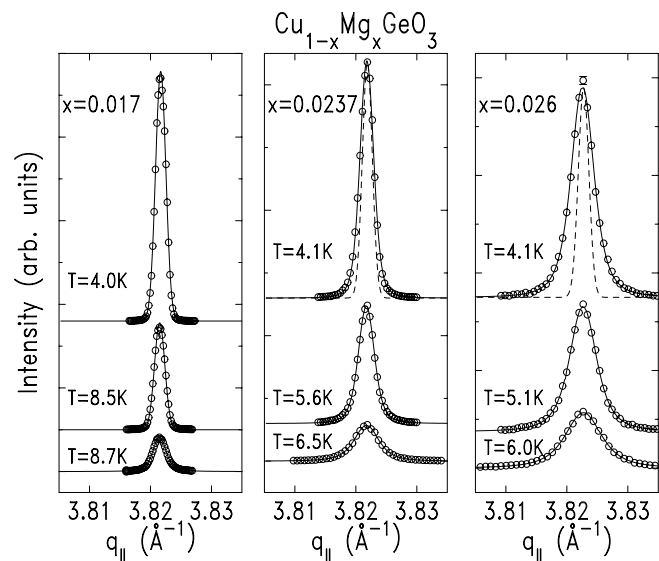


FIG. 1. Representative longitudinal scans at the (1.5, 1, 1.5) SP dimerization peak position. The solid lines are the results of fits as discussed in the text. The instrumental resolution function is shown as a dashed line.

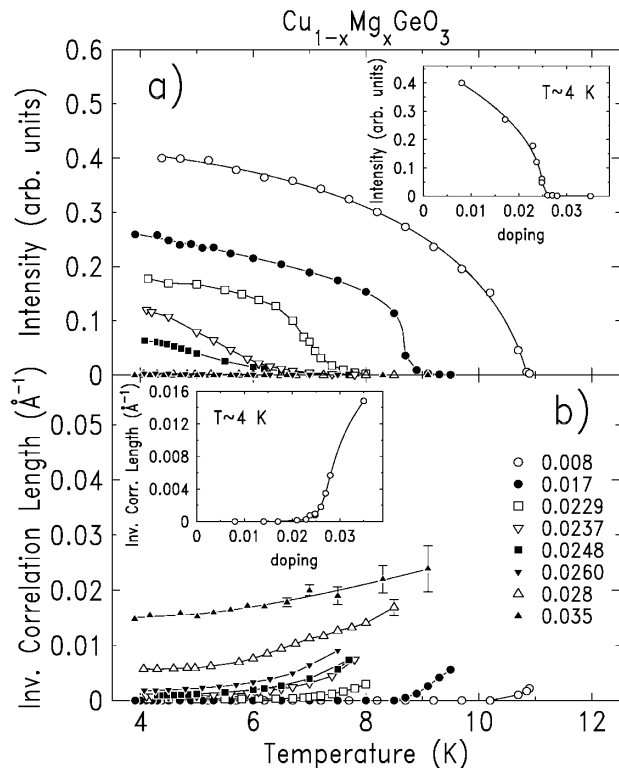


FIG. 2. The (1.5, 1, 1.5) SP peak intensity (a) and the corresponding inverse correlation length (b) as functions of temperature for various Mg-doping concentrations. Insets show the impurity-concentration dependence of the low-temperature SP peak intensity (a), and the corresponding inverse correlation length (b). The solid lines are guides to the eye.

former technique. If, as in the neutron experiment, we plot the SP peak intensity integrated over the corresponding broad momentum-space resolution volume [13], we obtain an apparent transition temperature which is much higher than the one evinced by the data of Fig. 3. Qualitatively, this can be seen from the data of Fig. 3 by taking into account the typical resolution of a neutron scattering experiment ($0.003\text{--}0.005 \text{ \AA}^{-1}$) and the fact that the integrated intensity is roughly equal to the product of the peak intensity and the two in-plane peak widths. Thus, the putative SP transition temperature found in the diffraction experiments from the SP peak intensity depends on the instrumental resolution. However, the transition temperature can be consistently determined as the temperature at which the system attains LRO as deduced from high-resolution x-ray measurements. Susceptibility measurements determine the temperature T_m at which a local spin gap appears [10] and this may or may not be simply related to the temperature at which true long-range structural order occurs [14].

Unlike pure CuGeO_3 , doped samples exhibit anomalously large relaxation times resulting in marked thermal hysteresis. The hysteresis disappears if the data are taken sufficiently slowly. Typically, a 30 to 60 min wait at each temperature is enough to ensure the absence of measurable

hysteresis. The slow dynamics found in this system will be discussed in much more detail elsewhere [13].

We have carefully determined the impurity-concentration dependence of the temperature T_s at which the LRO is achieved. The experiments were performed slowly enough to ensure the absence of measurable thermal hysteresis. The results, together with the susceptibility measurements of Ref. [5], are presented in the revised phase diagram for $\text{Cu}_{1-x}\text{Mg}_x\text{GeO}_3$ shown in Fig. 4. The error bars in Fig. 4 include possible beam heating effects estimated in Ref. [13]. These beam heating effects may also result in a small renormalization of the temperature scale in Figs. 2 and 3. Two characteristic temperatures, both related to the SP transition but defined by the physics on different length scales, are found in the doped material. At the higher temperature, T_m , the magnetic susceptibility and other thermodynamic probes, such as specific heat, exhibit an anomaly reflecting the opening of a local magnetic gap at T_m [10]. While at high x these probes give large uncertainties in the value for T_m , low resolution diffraction probes indicate the appearance of the lattice dimerization at about the same temperature, providing additional evidence for the local opening of the magnetic gap. As discussed above, we find that this lattice dimerization around T_m has a finite correlation length. The LRO is attained at a lower temperature T_s , at which no significant anomaly in the magnetic susceptibility is found. Thus, the following chain of events occurs with decreasing temperature. First, at $T = T_m$ local dimerization occurs and the magnetic gap opens up in finite-sized domains which presumably extend between individual Mg^{2+} dopants. As the temperature decreases and the 3D interactions favoring the SP state become relatively more important, the individual domains between the random

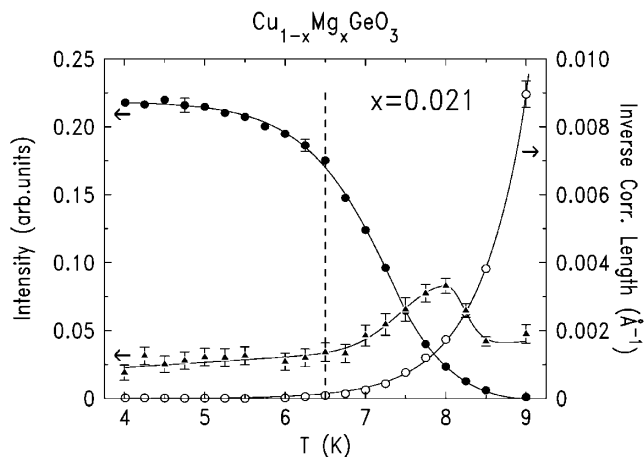


FIG. 3. The temperature dependences of the (1.5, 1, 1.5) SP peak intensity (filled circles), the intensity at the wing ($\Delta q = 4.5 \times 10^{-3} \text{ \AA}^{-1}$) of the SP peak (filled triangles), and the corresponding longitudinal inverse correlation length (open circles) in the $x = 0.021$ sample. The dashed line indicates the temperature at which, to the accuracy of our experiment, the long-range order is achieved. The solid lines are guides to the eye.

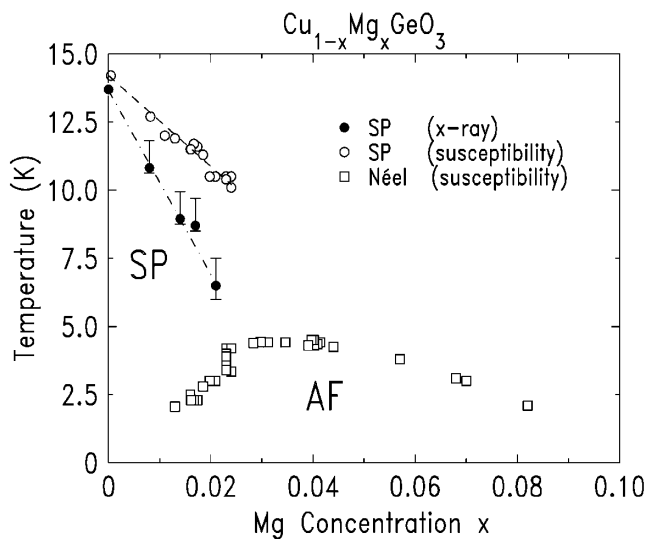


FIG. 4. The revised temperature-doping phase diagram of $\text{Cu}_{1-x}\text{Mg}_x\text{GeO}_3$. The filled circles indicate the temperature T_s at which the SP long-range order is achieved as determined in our experiment. The open circles show the SP transition temperature T_m as inferred from magnetic susceptibility measurements, and the squares show the Néel temperature [5].

Mg^{2+} dopants on different chains begin to correlate with each other over large distances, and 3D LRO is eventually achieved at $T = T_s$. Since this process involves only local rearrangement in the phase of the dimerization, no significant anomaly in thermodynamic variables is expected at T_s . We should emphasize that we cannot rigorously exclude the scenario in which for $x < x_c$ the low-temperature SP correlation length saturates at some finite value which is larger than our resolution limit of $0.5 \mu\text{m}$. In this case, T_s would be characterized as a long-distance crossover temperature rather than a true second order phase transition temperature.

The rich and complex properties exhibited by doped CuGeO_3 clearly cannot be explained by simple dilution effects alone. In fact, our data suggest that the SP “transition” in the doped material cannot be described as a conventional equilibrium phase transition. The severe rounding of the transition, the 3D Lorentzian-squared peak shapes, and the anomalously slow dynamics found in $\text{Cu}_{1-x}\text{Mg}_x\text{GeO}_3$ closely resemble analogous phenomena found in disordered systems with competing fields or interactions, such as the RFIM compounds [15], and spin glasses [16]. We believe that the resemblance of doped CuGeO_3 to systems with competing interactions or fields is not coincidental. As first argued by Harris *et al.* [17], the SP system can be mapped onto an effective 3D Ising model, in which the two dimer configurations possible in a given chain are associated with the up and down states of the Ising spins. The interchain interaction keeps the spin-chain dimerizations in phase. When a Cu atom is replaced by Mg in an isolated chain, it is energetically favorable for the Ising pseudospin direction to change sign

across the impurity since the Mg ion makes one of the original dimer configurations energetically unfavorable. Concomitantly, because the interchain interaction favors all pseudospin-up (or all pseudospin-down) configurations, introduction of impurities creates frustration in the 3D system. This is analogous to the situation in 3D Ising systems with mixed ferromagnetic and antiferromagnetic bonds although the appropriate pseudospin model needed to describe $\text{Cu}_{1-x}\text{Mg}_x\text{GeO}_3$ must be more elaborate, since one must consider explicitly the differences in behavior of even and odd number Cu^{2+} 1D spin segments as well as higher order random field effects. We will discuss this model much more extensively in Ref. [13]. At the minimum, it is clear that competing interactions are intrinsic to the doped CuGeO_3 system and must be included in any realistic model describing this compound [18].

We are grateful to G. Shirane, Y. Fujii, J.P. Hill, L.D. Gibbs, and A. Aharony for important discussions. We thank S. LaMarra for assistance with the experiments. This work was supported by the NSF under Grant No. DMR97-04532. This work was also supported by NEDO International Joint Research Grant, and by Grant-in-Aid for COE Research “SCP Coupled System” from the Ministry of Education, Science, Sports, and Culture of Japan.

- [1] For a review, see J.W. Bray *et al.*, in *Extended Linear Chain Compounds*, edited by J.C. Miller (Plenum, New York, 1982).
- [2] M. Hase *et al.*, Phys. Rev. Lett. **70**, 3651 (1993).
- [3] M. Hase *et al.*, Phys. Rev. Lett. **71**, 4059 (1993).
- [4] J.-G. Lussier *et al.*, J. Phys. Condens. Matter **7**, L325 (1995); M. Hase *et al.*, Physica (Amsterdam) **215B**, 164 (1995); S.B. Oseroff *et al.*, Phys. Rev. Lett. **74**, 1450 (1995); J.P. Schoeffel *et al.*, Phys. Rev. B **53**, 14971 (1996).
- [5] T. Masuda *et al.*, Phys. Rev. Lett. **80**, 4566 (1998).
- [6] K. Manabe *et al.*, Phys. Rev. B **58**, R575 (1998).
- [7] V. Kiryukhin *et al.*, Phys. Rev. B **54**, 7269 (1996).
- [8] Y. Sasago *et al.*, Phys. Rev. B **54**, R6835 (1996); M.C. Martin *et al.*, *ibid.* **56**, 3173 (1997).
- [9] H. Nakao *et al.*, preprint cond-mat/9811324.
- [10] In fact, inelastic neutron scattering measurements are needed to establish opening of the magnetic gap unambiguously.
- [11] T. Masuda *et al.*, preprint cond-mat/9906130.
- [12] R.A. Cowley *et al.*, Z. Phys. B **58**, 15 (1984); U. Nowak and K.D. Usadel, Phys. Rev. B **46**, 8329 (1992).
- [13] V. Kiryukhin *et al.* (unpublished).
- [14] See also the discussion, in G.B. Martins *et al.*, Phys. Rev. B **54**, 16032 (1996).
- [15] R.J. Birgeneau, J. Magn. Magn. Mater. **177–181**, 1 (1998).
- [16] See, *e.g.*, J.A. Mydosh, *Spin Glasses: an Experimental Introduction* (Taylor & Francis, London, 1993).
- [17] Q.J. Harris *et al.*, Phys. Rev. B **52**, 15420 (1995).
- [18] M. Mostovoy and D. Khomskii, Z. Phys. B **103**, 209 (1997).